Phototactic personality in fruit flies and its suppression by serotonin and *white*

Jamey S. Kain, Chris Stokes, and Benjamin L. de Bivort[1]

The Rowland Institute, Harvard University, Cambridge, MA 02142

Edited by Ulrike A. Heberlein, Howard Hughes Medical Institute, Ashburn, VA, and approved October 18, 2012 (received for review July 13, 2012)

Drosophila **typically move toward light (phototax positively) when startled. The various species of *Drosophila* exhibit some variation in their respective mean phototactic behaviors; however, it is not clear to what extent genetically identical individuals within each species behave idiosyncratically. Such behavioral individuality has indeed been observed in laboratory arthropods; however, the neurobiological factors underlying individual-to-individual behavioral differences are unknown. We developed "FlyVac," a high-throughput device for automatically assessing phototaxis in single animals in parallel. We observed surprising variability within every species and strain tested, including identically reared, isogenic strains. In an extreme example, a domesticated strain of *Drosophila simulans* harbored both strongly photopositive and strongly photonegative individuals. The particular behavior of an individual fly is not heritable and, because it persists for its lifetime, constitutes a model system for elucidating the molecular mechanisms of personality. Although all strains assayed had greater than expected variation (assuming binomial sampling), some had more than others, implying a genetic basis. Using genetics and pharmacology, we identified the metabolite transporter White and *white*-dependent serotonin as suppressors of phototactic personality. Because we observed behavioral idiosyncrasy in all experimental groups, we suspect it is present in most behaviors of most animals.**

ethology | stochasticity | bet-hedging | Ischnopterapion virens

Few debates in biology have generated broader interest than nature versus nurture. Not surprisingly, both heritable and environmental factors play significant roles in shaping an organism's traits. However, the precise contributions of genetic and environmental factors to complex traits, such as most behaviors, are poorly understood. Behavioral individuality, in the absence of genetic variation, has indeed been observed in the laboratory. Specifically, clonal pea aphids were shown to vary in their predator escape behavior, and these differences were maintained for at least 5 d (1). In another example, the naïve odor preference of fruit flies was highly variable across individuals (2). These experiments suggest that even when deterministic influences from genetics and environment are held constant, there is nevertheless considerable behavioral variability. *Drosophila* is an ideal model system to test whether individuals, matched both genetically and environmentally, possess unique behavioral personalities, and what genetic and neurobiological factors control the magnitude of this idiosyncrasy.

To determine whether individuals are behaving idiosyncratically we need to measure the trial-to-trial variation in an individual's behavior and compare that to the variation between individuals. If we observe greater variability between individuals than within individuals (that cannot be explained by sampling error), this would constitute evidence for behavioral idiosyncrasy. This analysis requires many trials per individual across many individuals. To explore and quantify the extent of variation in a simple behavior, we built FlyVac, an automated device to test the startled phototaxis behavior of many individual flies in parallel.

Results

Rapid Quantification of Phototaxis Behavior in Individual Flies Using FlyVac. Operation of FlyVac begins by loading individual flies into separate behavioral modules, each containing a phototactic T-maze in which one choice tube leads to a lit light-emitting diode (LED) (Fig. 1*A*, Fig. S1 *A* and *B*, and Movie S1). After a fly enters the maze and makes a choice, FlyVac (*i*) records the direction of the choice, (*ii*) randomizes the light and dark stimulus LEDs, and (*iii*) sends vacuum pulses to the module. These pulses whisk the fly back into the start tube of the T-maze (initiating a new trial), where an injury-mitigating "vacuum trap" catches the fly on a cushion of air (Fig. 1 *B* and *C*, Fig. S1 *C* and *D*, and Movie S2).

During testing, individual flies generally did not display learning or adaptation with respect to their light-choice probability (Fig. 1*D* and Fig. S1 *E* and *F*), which was not surprising given that they experience vacuum pulses irrespective of their phototactic choices. However, they did display adaptation in the form of increasing latency between completed trials (Fig. 1*D*). Importantly, the light-dark choice of a fly for any particular trial was essentially uncorrelated to its previous choice (the mutual information between successive trials, averaged across individuals, of the wild-type strain Canton-S, was 0.017 ± 0.0013 bits, on a scale of 0–1). Thus, we were able to treat all choices as statistically independent and by assaying large numbers of individuals many times each (40 trials, chosen arbitrarily; Dataset S1), we were able to quantify the individual-to-individual variation in phototaxis for any given strain.

All Strains Exhibit More Behavioral Variability than Expected by Chance Alone. We first investigated the phototactic behavior of the laboratory wild-type *Drosophila melanogaster* strain Canton-S. As expected, these animals were photopositive, choosing the light 80% of the time, on average (Fig. 1 *E* and *F*). The distribution of observed light-choice probabilities was superficially similar to what we expected from a population composed of animals with identical light-choice probabilities. However, some animals displayed very unlikely behaviors (Fig. 1*F*). For example, 1 animal (of 176 tested) chose the light 40 of 40 times ($P = 0.023$, corrected for multiple comparisons, assuming that light is chosen with a probability equal to the population mean). Another laboratory strain, *melanogaster* w^{1118} (null for the gene *white*, and the background strain for most transgenics) displayed lower average preference (61%) but, strikingly, had a much broader distribution of light-choice probabilities (Fig. 2*A*) than would be expected by chance if all animals were choosing light 61% of the time [$P < 10^{-10}$ by χ^2 test of variance; $P < 0.001$ by interquartile range (IQR) comparison]. We determined the expected distribution of observed light-choice probabilities by assuming that each fly chooses light with a probability equal to the fraction of all choices made by that strain that were photopositive. Because successive trials were effectively independent, the distribution of outcomes under this assumption can be modeled by binomial distributions, with parameters n_i indicating the number of trials completed by each fly.

Author contributions: J.S.K. and B.L.d.B. designed research; J.S.K. and B.L.d.B. performed research; J.S.K., C.S., and B.L.d.B. contributed new reagents/analytic tools; J.S.K. and B.L.d.B. analyzed data; and J.S.K. and B.L.d.B. wrote the paper.

The authors declare no conflict of interest.

This article is a PNAS Direct Submission.

Freely available online through the PNAS open access option.

[1]To whom correspondence should be addressed. E-mail: debivort@rowland.harvard.edu.

This article contains supporting information online at www.pnas.org/lookup/suppl/doi:10.1073/pnas.1211988109/-/DCSupplemental.

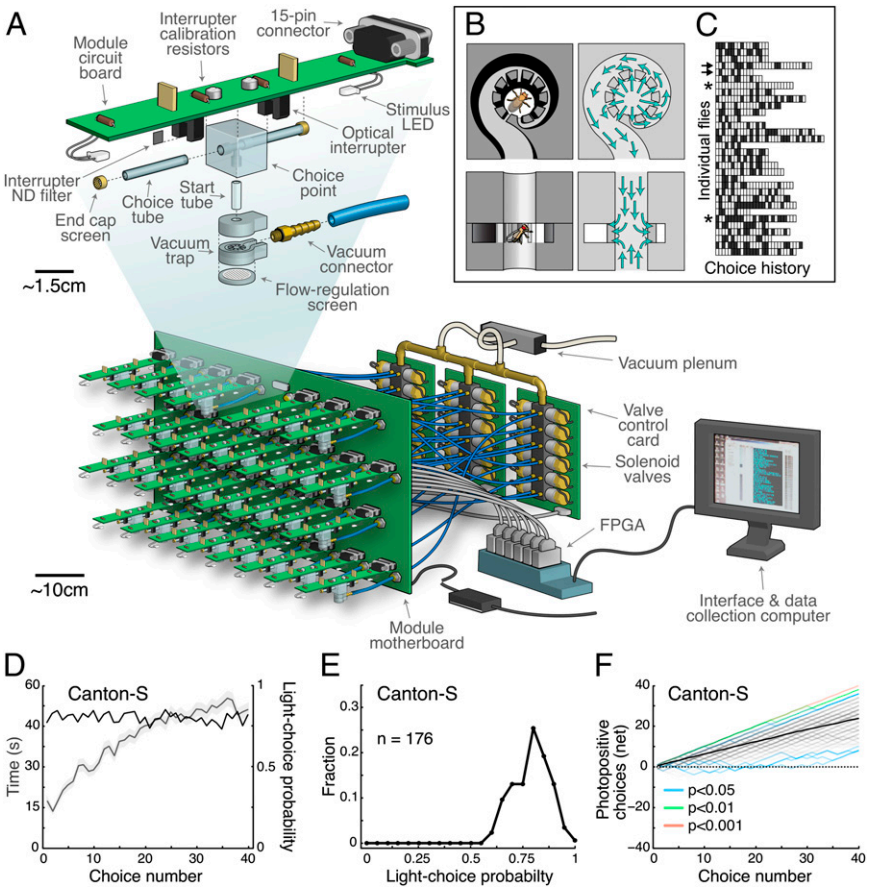

Fig. 1. Automatic phototactic behavior assay device FlyVac and wild-type phototactic behavior. (*A*, *Upper*) Single FlyVac module with a phototactic T-maze. Flies are loaded into the start tube and climb to the choice point where the stimulus LEDs become visible. In each trial, one LED is lit at random. After committing to a choice tube and crossing an infrared beam, the vacuum line associated with this module opens and the fly is pulled back to vacuum trap at the end of the start tube. (*A*, *Lower*) FlyVac motherboard with 32 individual phototaxis modules connected, control processor field programmable gate array (FPGA), and vacuum infrastructure (also see Movie S1 and Fig. S1). (*B*) Cross-sectional schematics of air-cushioning vacuum trap (*Left*), with airflow pattern (*Right*). Flies are pulled into the trap by air flowing down from the choice tubes and up from the bottom opening of the vacuum trap. Thus, the trap catches the flies on a cushion of air, mitigating damage (also see Movie S2). (*C*) Snapshot of typical data during a FlyVac session. Each row represents a single fly in one of 32 modules, and flies make choices at their own respective pace. Black boxes indicate photonegative choices, white boxes indicate photopositive choices, asterisks indicate flies with evidently different light-choice probabilities, and arrows indicate flies with different choice rates. (*D*) Average trial completion time (gray) and average light-choice probability (black) across Canton-S flies versus trial number. Light gray shaded region indicates ±1 SE. (*E*) Histogram of light-choice probabilities across Canton-S individuals. (*F*) Net photopositive choices versus choice number for individual wild-type (Canton-S) flies. Dotted line indicates an equal number of light and dark choices. Black line indicates average trajectory across all flies. Colored trajectories indicate outcomes that are unlikely under the assumption that all flies choose light with the same probability. Two-tailed *P* values are calculated from the binomial distribution, uncorrected for multiple comparisons. The red trajectory is significant after Bonferroni correction ($P = 0.027$).

As a check that FlyVac itself was not introducing artifacts, we assayed w^{1118} animals with both stimulus LEDs on. In this situation, when the animal reaches the choice point, both choice stimuli are identical, but one of the two maze branches was designated, arbitrarily, to be the "light-positive" direction. As expected, the resulting distribution was statistically indistinguishable from the random binomial expectation (Fig. 2*B*). We also assayed blind *norpA* flies (3), and their behavioral distributions matched the random binomial expectation (Fig. 2*C*). Additionally, we verified that trial completion time, birth order, maternal identity, sex, reproductive status, and circadian rhythm had no, or negligible, effect on light-choice probability (Fig. S2 *A–F*).

The phenomenon of individual-to-individual variability was not restricted to domesticated *D. melanogaster* (Fig. 2 *D–H*). Indeed, strains of *D. simulans* and *D. pseudoobscura* exhibited the greatest behavioral variation. With the exception of control experiments (Fig. 2 *B* and *C*), every strain we tested exhibited variability beyond expectation (Fig. 2*G*). We even observed this phenomenon in insects of a different order: wild caught white clover weevils (Ischnopterapion virens), strongly suggesting that behavioral idiosyncrasy is ubiquitous.

The light-choice probability distributions of several strains were clearly not Gaussian, so we devised a nonparametric $\log_2$-linearized metric to quantify variability beyond expectation (VBE). On this scale, VBE = 0 indicates that the observed behavioral variability within a population equals the sampling variability expected of animals choosing light with identical probabilities (e.g., the blind *norpA* flies, with VBE not statistically distinct from 0). VBE = 1 indicates twice as much variability as expected, VBE = 2 four times as much, etc. VBE ranged from 0.35 for Cambridge-A (*D. melanogaster*) to 1.3 for *simulans* w^{501} (Fig. 2 *G* and *H*), 27% and 146% excess variability respectively. VBE was greater than zero in all noncontrol experiments ($10^{-93} < P < 0.007$ by χ^2, IQR, and *z* tests). *D. simulans* strains had higher VBE scores than most *D. melanogaster* strains, suggesting the magnitude of behavioral idiosyncrasy may vary between species. Notably, the average VBE of isogenic *D. melanogaster* strains (0.65) was greater than that of polygenic strains (0.43; $P = 0.045$ by *t* test). Furthermore, aggressively inbreeding the isogenic strain *D. melanogaster* w^{1118} for an additional 10 generations did not alter the VBE (Fig. 2 *G* and *H*), suggesting that genetic differences between individuals are unlikely to explain their idiosyncratic behaviors.

Behavioral Variability Constitutes a Form of Fly Personality. Next, we directly tested whether the idiosyncratic behavior of outlier flies is heritable. Starting with the isogenized and inbred $w^{1118\ (iso)}$ strain, we bred nine pairs of parents chosen from the tails of the original behavioral distribution. There was no evidence of heritability between the light-choice probability of the parental pairs and their respective progeny [Fig. 3*A*; mean $h^2 = 0.044 \pm 0.084$ by selection test of heritability (4)], reiterating that cryptic heritable variation does not explain the behavioral differences between individuals, nor consequently the VBE of the population. However, the magnitude of VBE varies between genetically distinct strains (Fig. 2), presumably due to loci polymorphic between strains but not within them.

Perhaps environmental variability, such as differing visual (5), nutritive (6), or social (7) experience, causes VBE. To test this, we reared animals singly, from eggs, in their own vials, in darkness. The VBE of these "environment-matched" animals was slightly reduced (Fig. 3*B*), but statistically indistinct from $w^{1118\ (iso)}$ animals ($P = 0.11$ by bootstrap resampling), and significantly greater than

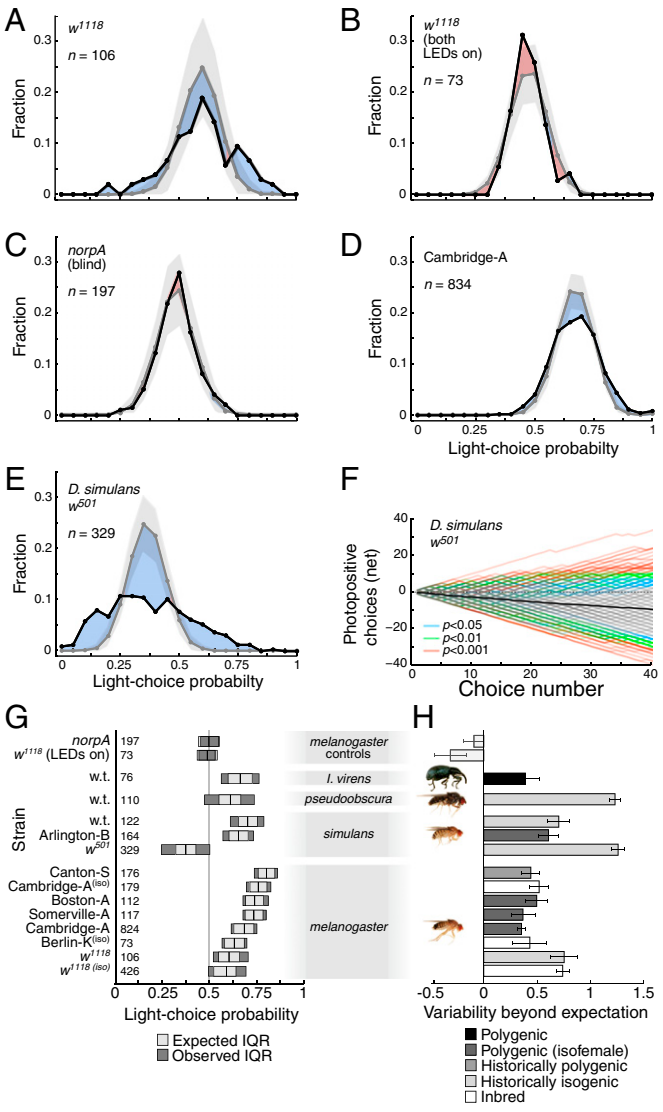

Fig. 2. Behavioral VBE is present in all tested *Drosophila* strains. (*A–E*) Observed light-choice probability histograms (black) superimposed over the distribution expected if all animals chose the light with identical probabilities (gray). Light gray regions indicate the 95% confidence interval of the expected distribution, given sampling error. Blue regions indicate evidence of individual-to-individual behavioral variability, red regions counter-evidence. In *B*, both stimulus LEDs were on during all trials, but one tube was designated, arbitrarily, to be the "photopositive" direction. (*C*) Blind flies follow the expected binomial distribution, indicating that nonvisual cues, such as olfactory or temperatures differences, are negligible with respect to choice behavior. (*F*) Light-choice trajectories for *simulans* w^{501}, as in Fig. 1*F*. (*G*) Observed (dark gray) and expected (light gray) light-choice probability IQRs for control groups and various wild types, by species. Numbers at left indicate sample size. See Table S1 for strain details. Labels and images in *H* indicate species. (*H*) For the same groups, metric indicating the amount of behavioral variability beyond statistical expectation (VBE). On a $\log_2$ scale, VBE = 0 indicates no excess variability, and VBE = 1 indicates twice as much variability as would be expected by chance alone. Shades of bars indicate the degree of polygenicity in each strain. Polygenic *Drosophila* lines were recently caught near Boston, MA, and cultured in the laboratory before testing. Wild clover weevils (*Ischnopterapion virens*) were caught and tested immediately. Error bars are ±1 SE as calculated by bootstrap resampling; all strains (other than controls) have VBE > 0 with $P < 0.007$ (by *z* test and VBE resampling).

zero ($P < 0.001$ by χ^2, IQR, and *z* tests). Thus, genetically identical animals, in very closely matched environmental conditions, still display much more behavioral variation than expected by sampling error alone.

We wondered whether the idiosyncratic behavior of an individual fly would remain if the animal was assayed again at later time points. Flies were assayed once at 5 d posteclosion and then again at one of several time points ranging from 1 d to 28 d later (Fig. 3*C* and Fig. S2*G*). The idiosyncratic behavior of each fly was partially preserved (i.e., dark-preferring flies remained dark-preferring) over at least 4 wk, essentially a fly lifetime. Thus, VBE can be interpreted as phototactic "personality" [sensu (1)].

***white* Gene Suppresses Behavioral Variability.** What molecular factors, if any, determine the extent of personality? Recall that every strain assayed displayed more variation than expected, and yet some had much more than others, suggesting a genetic underpinning (Figs. 2*H* and 4*A*). We observed that the w^{1118} strain showed the greatest VBE within *D. melanogaster* and, similarly, the VBE of *simulans* w^{501} was greater than that of the wild-type *D. simulans* strain. Both the w^{1118} and w^{501} alleles of *white* are loss of function mutations, rendering the animals white-eyed. Importantly, although they lack screening pigments and have reduced visual acuity (8), white-eyed *Drosophila* are not blind; they phototax positively (Fig. 2*A*) and have elevated personality; blind flies lack visual personality altogether (Fig. 2*C*).

To test whether *white* affects VBE, we moved the *simulans* mutant w^{501} allele of *white* into a wild-type genetic background by

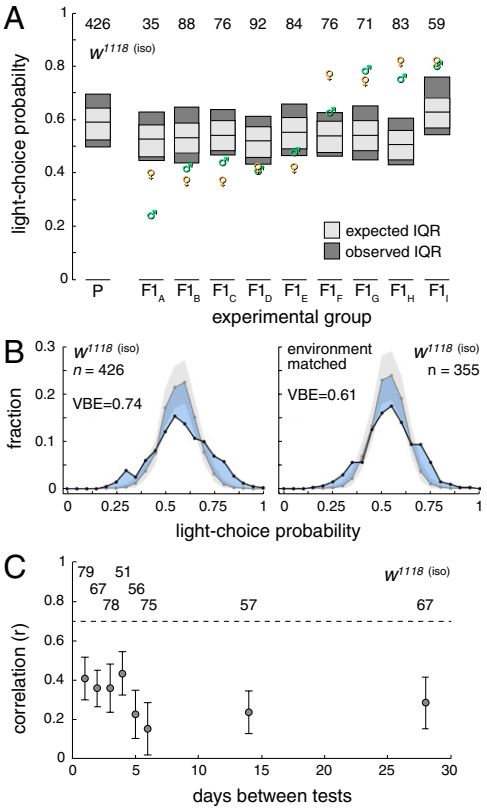

Fig. 3. Behavioral variability constitutes a form of nonheritable fly personality. (*A*) Expected (light gray) and observed (dark gray) light-choice probability IQRs of progeny (F1) populations derived from the mating of individual flies exhibiting unusual light-choice probabilities (male and female symbols). Numbers above indicate sample sizes. (*B*) Light-choice probability histograms for w^{1118} (iso) (as in Fig. 2 *A–E*) reared with and without strict environmental matching. (*C*) Correlation coefficient (*r*) of individual light-choice probabilities between first and second testings versus time interval between the tests. The dashed line indicates the upper bound on the correlation, given sampling error, and under the assumption that individual flies choose light in the second session with the probability they display in the first session. Error bars are ±1 SE, calculated by bootstrap resampling; numbers indicate sample sizes.

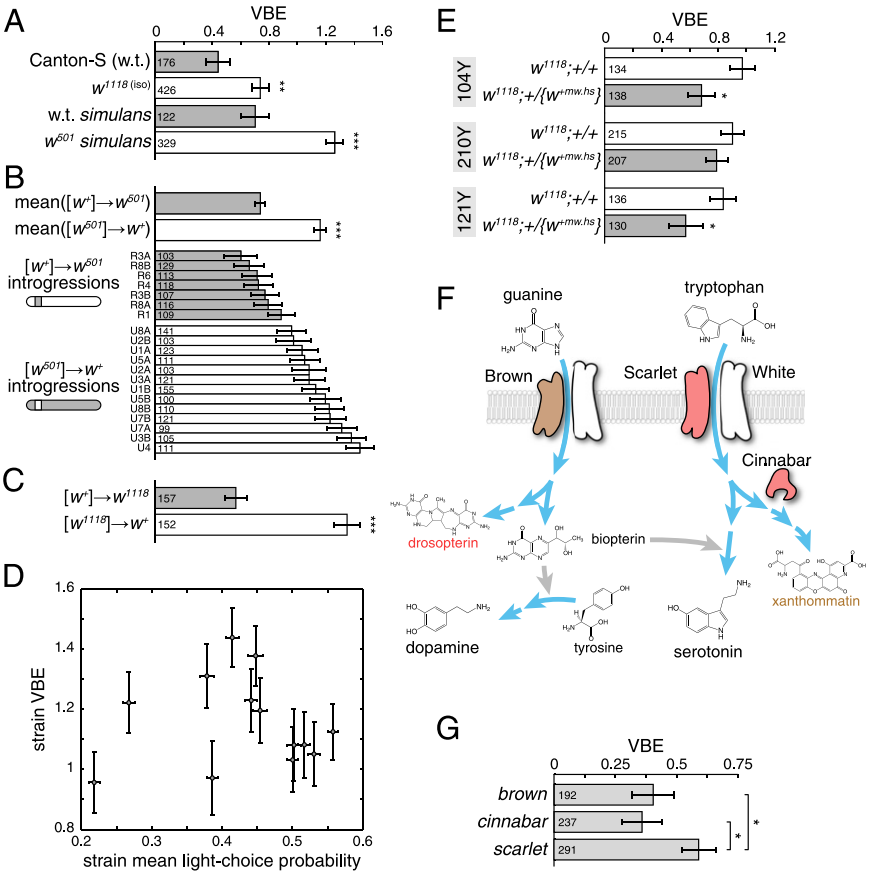

Fig. 4. The White pathway is required for wild-type personality levels. (*A*) Comparison of the VBE of w^- and wild-type *D. melanogaster* and *D. simulans* strains. Error bars are ±1 SE, calculated by bootstrap resampling; numbers in bars indicate sample sizes. $*P < 0.05$, $**P < 0.01$, $***P < 0.001$ comparing *white* mutants to their conspecific wild type. (*B*, upper two bars) Mean VBE of *D. simulans* lines in which the w^+ *allele* was introgressed into the background of the w^{501} strain for 10 generations, and vice versa. The mean VBEs of the introgression lines nearly fully recapitulate the VBEs of the parental *D. simulans* strains (*A*, lower two bars). Error bars are ±1 SEM. (*B*, lower bars) VBEs of individual introgression lines contributing to the means shown above. Error bars are ±1 SE, as calculated by bootstrap resampling; numbers are sample sizes. (*C*) VBEs of *D. melanogaster* $[w^{1118}]\rightarrow w^+$ and $[w^+]\rightarrow w^{1118}$ introgression lines. (*D*) VBE versus mean light-choice probability for the $[w^{501}]\rightarrow w^+$ introgression lines in *B*. Error bars are ±1 SEM (*x* axis) and ±1 bootstrapped SE (*y* axis). (*E*) VBEs of sibling flies either expressing (gray) or not expressing (white) the $white^+$ transgene under a constitutive promoter. $white^+$ transgenic strains 104Y and 121Y fully rescue low VBE in $w^{1118\ (iso)}$ genetic background animals (results and Table S1). Compare with upper two bars of *A*. The $white^+$ transgenic strain 210Y may partially rescue wild-type VBE. (*F*) Diagram of the role of White in importing precursors of dopamine, serotonin, and the eye pigments xanthommatin and drosopterin. Gray arrows indicate the role of biopterin as a cofactor. (*G*) VBEs of flies with mutations in the genes encoding the heterodimer partners of White, *brown* and *scarlet*, and the *cinnabar* gene, which encodes a pigment synthesis enzyme downstream of Scarlet but is not involved in serotonin biosynthesis.

introgression for 10 generations. We also reciprocally moved the $white^+$ allele into the mutant background. These two introgressions recapitulated the VBE seen in the original strains (Fig. 4*B*), suggesting *white* (or some closely linked locus) accounts for the entire difference. We repeated these introgressions in *D. melanogaster* as well, moving the *mutant* w^{1118} allele into the Canton-S wild-type and the $white^+$ allele into the mutant strain; the results were even more striking than the *D. simulans* experiment (Fig. 4*C*).

The independent *D. simulans* introgression lines were observed to have a wide variety of average light-choice probabilities that were statistically distinct (Fig. 4*D*), presumably because of their each having distinct recombination break points introduced by introgression, and, consequently, distinct polymorphisms affecting their light-choice probability. However, the associated VBEs of these lines were uncorrelated to light-choice probability ($r = -0.012$; $P = 0.97$). We conclude that although *white* mutants have reduced visual acuity and slightly reduced average light-choice probabilities (Figs. 4*D* and 2*G*), their greater VBE is not an artifact of either of these qualities.

Next, we set out to rescue the elevated VBE of the *white* mutant by backcrossing to $w^{1118\ (iso)}$ the transgenic $white^+$ strain 104Y (9) (which expresses $white^+$ constitutively in the w^{1118} background, as well as Gal4, which is incidental to this experiment). This backcross yielded a brood in which half of the siblings were null for the $white^+$ transgene, whereas the other half had a single copy. The $white^+$ heterozygotes had significantly reduced VBE compared with the nulls (Fig. 4*E*). We repeated this experiment using two additional $white^+$ transgenic strains (210Y and 121Y) and again found that the progeny with $white^+$ transgenes had lower VBE than their corresponding *white*-null siblings. The 13% reduction observed in 210Y was not statistically significant, perhaps because of weaker $white^+$ transgene expression; the 31% reduction in 121Y was significant ($P = 0.042$). Therefore, transgenic $white^+$ rescues the high personality of w^{1118} mutants.

Why would a gene in an eye pigment pathway affect personality? *white* encodes an ATP-binding cassette transporter that heterodimerizes with either the protein Brown or Scarlet to transport guanine or tryptophan, respectively (10), which are converted into the pigments drosopterin and xanthommatin, respectively. However, tryptophan is also a precursor of serotonin (11), whereas guanine is a precursor of biopterin, a cofactor involved in both serotonin and dopamine synthesis (12) (Fig. 4*F*). Indeed, *white* mutants have diminished concentrations of the neurotransmitters serotonin, dopamine, and histamine (13, 14) and concomitant behavioral phenotypes affecting courtship (15), spatial learning (16), and olfactory learning (17). To further investigate the role of *white*, we assayed the mutants *brown*, *scarlet*, and *cinnabar* (which encodes an enzyme in the xanthommatin synthesis pathway downstream of Scarlet but not in the serotonin synthesis pathway). The VBE of *scarlet* (Fig. 4*G*) was greater than that of either *brown* ($P = 0.048$) or *cinnabar*, ($P = 0.019$), suggesting a role for serotonin specifically (although these mutations were not in a common, recently isogenized background, so we cannot formally rule out another polymorphism).

White-Mediated Serotonin Suppresses Behavioral Variability. If serotonin is involved in regulating personality, pharmacological manipulation of serotonin levels should alter VBE. Feeding Canton-S adults α-methyl-tryptophan (aMW), a serotonin-synthesis inhibitor (18), increased VBE significantly (Fig. 5*A*). Conversely, feeding $w^{1118\ (iso)}$ animals 5-hydroxytryptophan (5HTP), a serotonin precursor, suppressed personality to a Canton-S-like level (Fig. 5*B*). Because 5HTP suppresses personality in the *white* mutant strain, we wondered whether it could further reduce VBE in wild-type animals. Canton-S flies fed 5HTP did not show a change in VBE (Fig. 5*A*), suggesting that there are limitations in the extent to which serotonin can suppress phototactic personality.

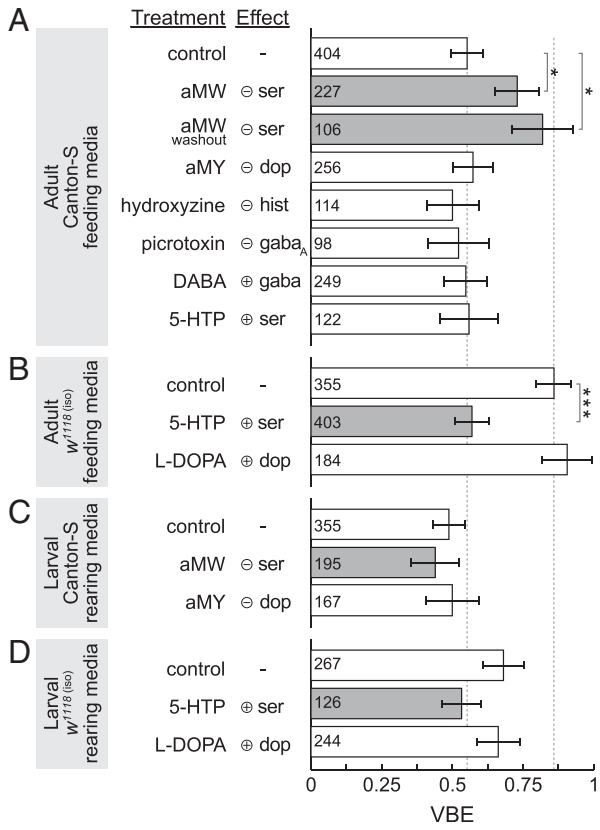

Fig. 5. Pharmacological manipulation of serotonin recapitulates wild-type and *white* VBE levels. (*A*) VBE of wild-type flies fed for 5 d posteclosion on media containing inhibitors of serotonin, dopamine, histamine, and GABA signaling: aMW, aMY, hydroxyzine, and picrotoxin, respectively. Serotonin inhibition increases VBE to the level of $w^{1118\ (iso)}$ mutants. GABA uptake inhibitor DABA and serotonin precursor 5HTP have no effect on wild-type VBE. Washout indicates flies fed aMW for 5 d, tested, fed control media for 5 d, and tested again. Error bars are ±1 SE. $*P < 0.05$; $***P < 0.001$. Numbers in bars indicate sample sizes; dotted lines are visual guides for wild-type and $w^{1118\ (iso)}$ mutant VBEs. (*B*) VBE of $w^{1118\ (iso)}$ flies fed the serotonin and dopamine precursors 5HTP and L-DOPA. 5HTP restores wild-type VBE levels. (*C* and *D*) VBEs of wild-type and $w^{1118\ (iso)}$ flies reared in culture media containing serotonin and dopamine inhibitors and precursors, exhibiting no effects compared with controls.

Because *white* mutation also reduces levels of dopamine and histamine (13), we fed inhibitors of these neurotransmitters [α-methyl-tyrosine (aMY) (19) and hydroxyzine (20), respectively] to wild-type animals and found no effect (Fig. 5*A*). Similarly, feeding *white* mutants the dopamine precursor L-3,4-dihydroxyphenylalanine (L-DOPA) had no effect. We also looked for a role for the inhibitory neurotransmitter γ-aminobutyric acid (GABA), which has been shown to tune olfactory behavioral responses (21) and is strongly expressed in the central complex (22), a region of the brain involved in stimulus choice behaviors (23). Synthesis of the inhibitory neurotransmitter GABA is *white*-independent, and we found that feeding flies picrotoxin, an antagonist of $GABA_A$ receptor channels (24), had no effect on VBE (Fig. 5*A*). DL-2,4-diaminobutyric acid (DABA), a selective inhibitor of the GABA uptake system, increases the GABA concentration in the synaptic cleft (25) but had no effect on the VBE of Canton-S flies. Finally, rearing larvae in either neurotransmitter precursors (5HTP or L-DOPA) or synthesis inhibitors (aMW or aMY) had no effect on the VBE of the resulting adults (Fig. 5 *C* and *D*). In summary, of the drugs we investigated, only those affecting serotonin modified behavioral variability and only when fed to adult flies.

Although the lack of response to a pharmacological agent cannot be taken as definitive evidence of no role for the corresponding neurotransmitter, these pharmacological experiments were based on previous treatments known to affect behavior. To confirm that the drugs were bioavailable in the fly brain, we examined two other behavioral features measured by FlyVac data: the group light-choice probabilities and group activity levels (as measured by the mean intertrial completion time). Each drug exerted a small, but highly significant effect (attributable to the large sample sizes generated by FlyVac) on at least one of these behavioral measurements (Fig. S3), indicating that they were bioavailable and had the potential to modify VBE. Thus, endogenous serotonin, but likely not dopamine, histamine, or GABA, suppresses phototactic personality, and exogenous serotonin can rescue the excessive personality levels of *white* mutants.

Discussion

Here, we examined the question of whether genetically identical animals raised in identical conditions exhibit behavioral variation. Using our high-throughput behavioral device FlyVac, we found that all strains of *Drosophila* displayed more variation than would be expected by chance alone, with animals that were improbably photopositive and photonegative. This variation beyond expectation could only be studied once large numbers of animals were assayed individually. To that end, we assayed 17,600 animals individually across all experiments (Dataset S1). The observed variation did not diminish after additional inbreeding; rather, the VBE of isogenic strains was greater than that of polygenic strains. Nor did VBE diminish after selectively breeding animals from the tails of the distributions. Thus, behavioral idiosyncrasy cannot be explained by cryptic genetic variation, unless it arose by de novo mutations (e.g., ref. 26) in all of these populations.

Although genetic variation within a strain cannot account for phototactic personality, the amount of behavioral variability between strains varied significantly, suggesting that genetic factors underlie differences in the magnitudes of variation. This led us to the gene *white* and its purported role as an importer of metabolic precursors of serotonin. Indeed, we reduced the extreme variation of *white* mutants by feeding them the serotonin precursor 5HTP as adults. Likewise, we increased the variation in wild-type adults by feeding them an inhibitor of serotonin biosynthesis. Feeding these drugs to larvae had no effect on behavioral variability. Because light-choice probability remained constant in experiments that altered variability, we conclude that serotonin signaling alters processes that diversify phototactic polarity, rather than phototactic polarity itself. We favor a model where developmental noise changes critical properties of the neural circuitry underlying phototactic polarity and that serotonin normally acts to counteract this noise in adults (Fig. 6). Such diversifying processes have been shown to act at both the level of neuronal wiring and physiology within arthropod brains (27, 28).

In the adult *Drosophila* brain, a relatively small number of neurons are serotonergic yet they arborize extensively throughout the

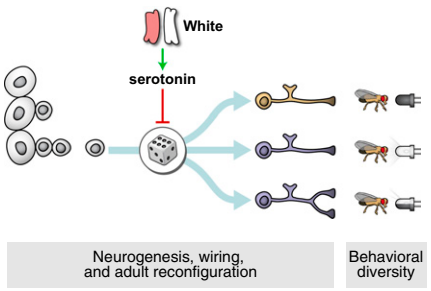

Fig. 6. Model of the regulation of phototactic personality by serotonin. During neurogenesis and wiring, developmental noise leads to wiring and/or physiological differences in the circuit controlling the polarity of phototaxis. Serotonin acts in adulthood to suppress the resulting behavioral variability.

brain (14, 29). Serotonin is detected in all neuropils of the optic lobes (lamina, medulla, lobula, and lobula plate) (29), including wide-field tangential neurons. Interestingly, the optic lobes of the larval CNS do not contain serotonin, which may explain why our drug treatments only affect VBE when treated as adults. Thus, serotonin is expressed in neurons capable of modulating the wide-field representation of visual information as well as higher order visual features.

The presence of personality in all tested *Drosophila* strains suggests it may be a universal phenomenon that should be investigated in other behavioral paradigms. For example, is there personality in chemotaxis or geotaxis? If so, any cross-modality correlation in the idiosyncratic behaviors of individually tested flies would indicate that the neuronal pathways underlying those behaviors are overlapping. That is, if unusually photopositive animals are also unusually negatively geotactic, we would predict shared elements in the neuronal pathways of these behaviors. One foreseeable challenge to the mechanistic study of personality in flies is an artifact of how most transgenic animals are generated, using ectopic *white*$^{+}$ as a marker for the insertion of the construct into a w^{1118} background. As we have shown, both genomic *white* mutations and ectopic *white* transgenes modify behavioral variability.

Nonheritable variation seems at first maladaptive, but perhaps it is tolerated as a pleiotropic consequence of other beneficial attributes. We propose three such possibilities. First, perhaps personality is the tradeoff for the rapid development of the boom-bust fruit fly (30); the developing brain is wired quickly but with some error. Second, perhaps the metabolic cost of complete suppression of personality is too high for the organism (31); it is advantageous to accept the presence of rare maladapted animals rather than bear the cost of additional regulatory pathways needed to develop with higher stereotypy. Third, perhaps personality is the byproduct of a neural circuit that is "balanced on a knife's edge" in terms of identifying a stimulus as attractive or aversive. Such a circuit would (*i*) generate a potentially advantageous mixed behavioral strategy (32) of, effectively at random, choosing to go toward the light with a particular average probability; (*ii*) be sensitive to any contravening stimuli, such as the appearance of a dragonfly; but also (*iii*) be sensitive to any small, intrinsic biases introduced by the neurons upstream of the circuit that resolves the phototactic decision. Alternatively, personality could be adaptive as a means of bet-hedging whereby variation that affects viability (but cannot be inherited) may allow outlier members of a species to survive acute transient stresses without altering the phenotypic distribution of their progeny.

Experimental Procedures

Insect Stocks. Clover weevils were caught by net and tested immediately. Flies were reared under standard growth conditions, except where otherwise noted. See *SI Experimental Procedures* for detailed rearing procedures and Table S1, indicating genotypes and sources for all strains used.

Pharmacology. Drugs were dissolved in Formula 4-24 instant *Drosophila* media (Carolina Biological Supply). For the drug-feeding, recently eclosed flies were transferred to vials of drug-containing media, incubated for 5 d, and then assayed. For drug-rearing, flies laid eggs in drug-containing media. Upon eclosion, drug-reared flies were transferred to drug-free food for 5 d and then assayed. See *SI Experimental Procedures* and Table S2 for drug protocols.

Statistical Analysis. Expected light-choice probability distributions were calculated analytically. VBE errors and hypothesis testing were performed by bootstrap analysis using custom scripts in MATLAB (MathWorks). See *SI Experimental Procedures* and Tables S3 and S4 for details.

ACKNOWLEDGMENTS. We thank Mike Burns, Andrew Speck, and Winfield Hill for technical advice; Don Rogers for assistance with fabrication; and Sam Kunes and Aravi Samuel for their extensive comments on analytic methods. Mike Burns, Sean Buchanan, and Josh Chapman helped collect wild insects. This work is supported by the Rowland Junior Fellows Program.

1. Schuett W, et al. (2011) Personality variation in a clonal insect: the pea aphid, Acyrthosiphon pisum. *Dev Psychobiol* 53(6):631–640.
2. Claridge-Chang A, et al. (2009) Writing memories with light-addressable reinforcement circuitry. *Cell* 139(2):405–415.
3. Bloomquist BT, et al. (1988) Isolation of a putative phospholipase C gene of Drosophila, norpA, and its role in phototransduction. *Cell* 54(5):723–733.
4. Fisher RA (1918) The correlation between relatives on the supposition of Mendelian inheritance. *Trans R Soc Edinb* 52:399–433.
5. Zhou M, et al. (2010) NMDA receptors-dependent plasticity in the phototaxis preference behavior induced by visual deprivation in young and adult flies. *Genes Brain Behav* 9(3):325–334.
6. Sharon G, et al. (2010) Commensal bacteria play a role in mating preference of Drosophila melanogaster. *Proc Natl Acad Sci USA* 107(46):20051–20056.
7. Yurkovic A, Wang O, Basu AC, Kravitz EA (2006) Learning and memory associated with aggression in Drosophila melanogaster. *Proc Natl Acad Sci USA* 103(46): 17519–17524.
8. Kalmus H (1943) The optomotor responses of some eye mutants of Drosophila. *J Genet* 45:206–213.
9. Yang MY, Armstrong JD, Vilinsky I, Strausfeld NJ, Kaiser K (1995) Subdivision of the Drosophila mushroom bodies by enhancer-trap expression patterns. *Neuron* 15(1): 45–54.
10. Nolte DJ (1952) The eye-pigmentary system of Drosophila. III. The action of eye-colour genes. *J Genetics* 51(1):142–185.
11. Joh TH (1997) Tryptophan hydroxylase: Molecular biology and regulation. *Handb Exp Pharmacol* 129:117–129.
12. Goodwill KE, Sabatier C, Stevens RC (1998) Crystal structure of tyrosine hydroxylase with bound cofactor analogue and iron at 2.3 A resolution: self-hydroxylation of Phe300 and the pterin-binding site. *Biochemistry* 37(39):13437–13445.
13. Borycz J, Borycz JA, Kubów A, Lloyd V, Meinertzhagen IA (2008) Drosophila ABC transporter mutants white, brown and scarlet have altered contents and distribution of biogenic amines in the brain. *J Exp Biol* 211(Pt 21):3454–3466.
14. Sitaraman D, et al. (2008) Serotonin is necessary for place memory in Drosophila. *Proc Natl Acad Sci USA* 105(14):5579–5584.
15. Zhang SD, Odenwald WF (1995) Misexpression of the white (w) gene triggers male-male courtship in Drosophila. *Proc Natl Acad Sci USA* 92(12):5525–5529.
16. Diegelmann S, Zars M, Zars T (2006) Genetic dissociation of acquisition and memory strength in the heat-box spatial learning paradigm in Drosophila. *Learn Mem* 13(1):72–83.
17. Anaka M, et al. (2008) The white gene of Drosophila melanogaster encodes a protein with a role in courtship behavior. *J Neurogenet* 22(4):243–276.
18. Dierick HA, Greenspan RJ (2007) Serotonin and neuropeptide F have opposite modulatory effects on fly aggression. *Nat Genet* 39(5):678–682.
19. Neckameyer WS (1996) Multiple roles for dopamine in Drosophila development. *Dev Biol* 176(2):209–219.
20. Shaw PJ, Cirelli C, Greenspan RJ, Tononi G (2000) Correlates of sleep and waking in Drosophila melanogaster. *Science* 287(5459):1834–1837.
21. Root CM, et al. (2008) A presynaptic gain control mechanism fine-tunes olfactory behavior. *Neuron* 59(2):311–321.
22. Hanesch U, Fischbach K-F, Heisenberg M (1989) Neuronal architecture of the central complex in Drosophila melanogaster. *Cell Tissue Res* 257(2):343–366.
23. Baker DA, Beckingham KM, Armstrong JD (2007) Functional dissection of the neural substrates for gravitaxic maze behavior in Drosophila melanogaster. *J Comp Neurol* 501(5):756–764.
24. Leal SM, Kumar N, Neckameyer WS (2004) GABAergic modulation of motor-driven behaviors in juvenile Drosophila and evidence for a nonbehavioral role for GABA transport. *J Neurobiol* 61(2):189–208.
25. Leal SM, Neckameyer WS (2002) Pharmacological evidence for GABAergic regulation of specific behaviors in Drosophila melanogaster. *J Neurobiol* 50(3): 245–261.
26. Muotri AR, et al. (2005) Somatic mosaicism in neuronal precursor cells mediated by L1 retrotransposition. *Nature* 435(7044):903–910.
27. Bucher D, Prinz AA, Marder E (2005) Animal-to-animal variability in motor pattern production in adults and during growth. *J Neurosci* 25(7):1611–1619.
28. Chou YH, et al. (2010) Diversity and wiring variability of olfactory local interneurons in the Drosophila antennal lobe. *Nat Neurosci* 13(4):439–449.
29. Vallés AM, White K (1988) Serotonin-containing neurons in Drosophila melanogaster: development and distribution. *J Comp Neurol* 268(3):414–428.
30. Félix MA, Braendle C (2010) The natural history of Caenorhabditis elegans. *Curr Biol* 20(22):R965–R969.
31. Laughlin SB, van Steveninck RRR, and Anderson JC (1998) The metabolic cost of neural information. *Nature Neurosci* 1(1):36–41.
32. Von Neumann J (1928) Zur theorie der gesellschaftsspiele. *Mathematische Annalen* 100(1):295–320.

Supporting Information

Kain et al. 10.1073/pnas.1211988109

SI Experimental Procedures

Apparatus Overview and Fabrication. Inside FlyVac, each fly proceeds upward under negative geotaxis into the choice point at which it is presented with one illuminated and one nonilluminated stimulus LED. Shortly after committing to move toward one LED or the other by moving into one of the choice tubes, the fly breaks the infrared beam of the corresponding optical interrupter. This signal is passed on to the control field programmable gate array (FPGA) unit, which (*i*) records the direction of the choice with respect to the illuminated LED; (*ii*) opens the solenoid valve associated with that module, pulling the fly back into the start tube; and (*iii*) illuminates exactly one of the stimulus LEDs at random.

Layout of the module and motherboard circuits was done using P-CAD software (Altium). All circuit boards are two-layer, 1-ounce copper-clad boards made from an FR-4 laminate, 1.57-mm thick, and were manufactured by Advanced Circuits. Power supply to the motherboard was a 23-W ac-to-dc adapter generating 12 and 5 V (no. SW20; Ault). Stimulus LEDs were 5,000 mcd, 7,700K white LEDs (no. LTW-420D7; Lite-On); the current going to them was regulated using a 56-ohm resistor. New designs would be advised to use a larger valued resistor on the order of 200 ohm, depending upon specific LED selected. The detectors of the optical interrupters (900-nm infrared; no. GP1A58HRJ00F; Sharp Microelectronics) were made more sensitive to small changes in emitter intensity by the insertion of two layers of 0.8-OD neutral density filter. These filters were custom printed on acetate using a black laser printer. The current through the interrupter emitters was tuned specifically for each interrupter, so that the passage of a fly through the interrupter was assured of triggering it, using a fixed 100-ohm resistor and a 100-ohm trimming potentiometer.

Choice tubes 26 mm long were made of clear nylon tubing (outer diameter, 3.18 mm; no. 8359K11; McMaster-Carr). The ends of each choice tube were capped with a porous screen of thin nylon mesh (black pantyhose), which allowed for airflow and light to pass through and, importantly, did not reflect light from the distal illuminated LED. Start tubes 16.5 mm long were made from 1-mL polystyrene pipettes (no. 414004-264; VWR), roughened to a matte finish on the interior. Choice point cubes and vacuum traps (Fig. 1*A* and Fig. S1*C*) were assembled from clear 5.3-mm-thick clear acrylic cut using an Epilog laser engraver. Flow-regulating screens, made of cotton fabric and reducing the airflow rate through a 2-mm tube from 440 cm^3/min by 50%, were held in place across the lower opening of each vacuum trap with a retaining acrylic ring. Vacuum traps were connected to Push-Quick motherboard fittings by latex and urethane tubing. Vacuum to each module was controlled by 12-V, two-way solenoid valves (no. EC-2M-12-H; Clippard) mounted to manifold/electronic control card (no. EMC-12-12-22; Clippard). This manifold was connected to a 754-cm^3 plenum to dampen drops in vacuum pressure when multiple solenoids opened in rapid succession. This was, in turn, supplied with a house vacuum that cycled from −15 to −22 inches of Hg.

Computer Interface and FPGA. Code for the CompactRio FPGA (National Instruments) was written in LabView (National Instruments), as was the interface program that records the behavioral data and allows manual manipulation of each module's stimulus LEDs and vacuum. During the operation, the FPGA ran at 1 MHz and examined each module ∼200 times per second. When an interrupter was tripped, the vacuum solenoid valve associated with that module was opened three times for 300 ms, separated by intervals of 300 ms. If an interrupter was tripped within 3 s of a prior tripping, it was assumed that the fly had not been dislodged by the prior vacuum pulses, and the vacuum pulses would be repeated. This contingency was not observed to occur during the operation of the device in its reported configuration. If a fly did not trip any interrupter for 120 s, it was pulsed three times with vacuum (as if it had tripped an interrupter) to keep the animal agitated. Signals output from the FPGA were mediated by 32 channel sinking digital-out CompactRio modules (no. 9477; National Instruments); inputs were mediated by 32-channel transistor-transistor logic digital-input/output modules (no. 9403; National Instruments).

FlyVac Operation. FlyVac operation proceeds as follows. Single flies are aspirated from storage vials containing standard fly media into the start tube of the T maze, the bottom of which can be accessed by removing the press-fitting vacuum trap. This trap (Fig. 1*B* and Fig. S1*C*) was inspired by the Francis turbine (1) but flowing in the opposite direction. Ten radial channels connect the interior of the start tube to a circumferential plenum with a diameter that increases to match the increasing flow contribution from each channel. This configuration creates a central region in which airflow pushes the fly from above and below, while pulling the fly simultaneously (with approximately equal flow) in all lateral directions (Movie S1 and Fig. S1*D*). As the fly deviates laterally from this unstable equilibrium, it restricts flow in the direction of that deviation, resulting in greater net flow in the opposite direction, thereby restoring its position in the center of the trap. Thus, relatively strong vacuum can be applied to the T-maze to reset the position of the animals without causing detrimental collision damage.

Upon leaving the trap, the fly proceeds upward under negative geotaxis (2) through the start tube into the choice point where it chooses to enter one of the choice tubes. Once it has moved 16 mm into a choice tube, it breaks the infrared beam of an optical interrupter. The sensitivity of each interrupter was tuned by trimming potentiometers, so that even small flies, off-center in the choice tubes would be detected. Breaking the beam of an interrupter signals (via the FlyVac motherboard) the FPGA controlling FlyVac to record the direction of that choice with respect to the direction of the illuminated stimulus LED and apply a series of three vacuum pulses to the vacuum trap, thereby resetting the fly into the start tube. Choice histories are recorded on a module by module basis (Fig. 1*C*), along with the corresponding history of stimulus directions and the time taken by the fly to complete each trial. Recording individuals for 40 trials was chosen somewhat arbitrarily; it is a compromise between three factors: (*i*) gathering sufficient data for analysis, (*ii*) waiting time until the next animal could be loaded, and (*iii*) ensuring that the large majority of animals would survive all trials without extensive physical damage. After completing 40 trials, the module is deactivated and the flies are simply contained until removal. In the event that a fly does not complete 40 trials within several hours, that fly is removed but the data are used if the animal had completed at least 10 trials.

Fly Stock Isolation and Maintenance. J. Dubnau (Cold Spring Harbor Laboratories, Laurel Hollow, NY) and W. Quinn (Massachusetts Institute of Technology, Cambridge, MA) provided stocks of w^{1118} and Canton-S flies, respectively. Other wild-type stocks and mutants were acquired from the Bloomington Stock Center at Indiana University. Local wild stocks were captured using fruit-baited traps, or, in the case of Somerville-A, by picking pupal cases from the margin of a compost pile. Single females from the Cambridge, Arlington, and Boston traps founded isofemale lines composing the Cam, Arl, and Bos stock series. The species iden-

tification of all wild stocks was confirmed by crossing them to *D. melanogaster* and *D. simulans* laboratory stocks. Clover stem weevils (*Ischnopterapion virens*) were chosen for experiments because they were nondipteran, of appropriate size for FlyVac, and locally abundant. They were collected by net from clover in the North Point Park (Cambridge, MA).

All lines were propagated using standard *Drosophila* culture methods on Caltech cornmeal media (BuzzGRO brand; Scientiis) in 25 °C humidity-controlled incubators set to a 12-h dark/12-h light cycle. Before most experiments, parental adults were segregated by sex and transferred to new food vials. Progeny were isolated at eclosion and stored in new vials for 5–10 d before testing. In general, most animals were assayed on day 5 posteclosion.

For the Cambridge-A circadian experiments, ∼30 separate vials were used to grow ∼1,100 total progeny generation animals aged 1–4 d since eclosion. These were then mixed, portioned into new vials containing 20 males or 20 females, allowed to age 4 d, and only removed from the incubator and light cycle immediately before testing in FlyVac. For the w^{1118} circadian experiments, age-matched males and females were assayed at four time points (zeitgeber −1, +5, +11, and +17) 5 d posteclosion. As before, flies were only removed from the incubator and light cycle immediately before testing in FlyVac.

For the environment-matched experiment, parental egg-laying proceeded as normal, but individual eggs were picked under the dissecting scope and placed alone on the surface of the media in fresh vials. These single-egg vials were placed in light-blocking, ventilated boxes and incubated until they contained 5-d posteclosion adults from which ∼30 random pairs of 1 male and 1 (virgin) female were allowed to breed under normal conditions in separate tubes containing KimWipes (Kimberly-Clark) as an egg-laying substrate. On a daily basis thereafter, the KimWipes in each breeding tube were replaced, with any oviposited eggs being transferred to the surface of media in individual tubes, as above. These batches of eggs were allowed to mature in the dark into 5-d posteclosion adults as above, which were then tested in FlyVac. Thus, both the experimental group and their parents were raised under the same, environment-matched conditions.

Drug Treatments. For aMW, aMY, 5HTP, L-DOPA, DABA, picrotoxin, and hydroxyzine feeding experiments, animals were reared on standard media until they had eclosed, at which point they were transferred to potato media containing the drug (or no drug, in the case of controls) for 5 d before testing (Table S2). aMW media (and its control media) were supplemented with ascorbic acid as a stabilizer. Control groups with unsupplemented or ascorbic acid-only supplemented media yielded animals with essentially identical VBEs and light-choice probabilities and were merged for analysis. For rearing experiments, adults were incubated on potato media supplemented with the appropriate drug for 5 d, at which point they were removed (often to be assayed in FlyVac, otherwise into the morgue). When their progeny eclosed, they were removed in the first 24-h posteclosion, anesthetized, separated by sex, and moved to standard media for 5 d before testing. In drug-washout experiments, flies were (*i*) placed on standard food until 0–24 h posteclosion, (*ii*) transferred to potato media plus drug for 5 d, (*iii*) tested in FlyVac for up to 2 h (or 40 trials, whichever was faster), (*iv*) placed into individual tubes per fly of standard media for 5 d, and (*v*) tested a second time in FlyVac.

Drug concentrations were chosen based on the *Drosophila* literature (Table S2). 5HTP and aMY did not fully dissolve at their respective concentrations, and in these cases, we suspended all undissolved drug by heavy vortex mixing of the drug stock solutions before mixing with media powder.

Calculation of Expected Distributions. To calculate the expected distribution of phototactic indices for a particular population, we started with a binomial distribution with parameter P equal to the aggregated light choice probability across all animals tested in each experimental group. This choice is appropriate considering the two-outcome nature of the assay and the observation that there was essentially no mutual information between sequential choices (0.017 bits for Canton-S, 0.019 bits for $w^{1118\ (iso)}$, 0.0212 bits for Cambridge-A, etc.). However, it was inappropriate to use the binomial distribution "as is" because the number of completed trials varied between the animals making up that population. Therefore, for a given binning of possible indices, the expected distribution was calculated as the sum across all animals of $Bin(n_i, k_{i,b}, P)$, where Bin is the binomial function, n_i is the number of trials completed by that animal, $k_{i,b}$ is the number of light choices (given n_i) contributing to each bin b of the final distribution, and P is the aggregated light-choice probability of all animals in the population. The SD of observed distributions under the null hypothesis of uniform light-choice probability was calculated using the property that the variance of the sum of uncorrelated random variables is the sum of their variances, i.e., the sum across flies of $n_i \times P_{i,b} \times (1 - P_{i,b})$, where $P_{i,b} = Bin(n_i, k_{i,b}, P)$.

Statistical Comparison of Observed and Expected Distributions. Whether the observed distributions of phototactic scores were broader than expected was assessed three ways: (*i*) using the χ^2 test of variance (somewhat appropriate because most phototactic score distributions were approximately Gaussian); (*ii*) with a nonparametric statistic equal to the IQR of the observed phototactic scores. One-tailed P values for the IQR were approximated by repeatedly simulating n-matched distributions of phototactic indices under the null hypothesis of a light-choice probability identical across all animals and all trials and reporting the fraction of these simulated distributions IQRs greater than actually observed. For each P value reported, we performed 10^4 or $1000/P$ simulations, whichever was greater (e.g., if P was reported as 0.5, this was based on 10^4 simulations; if P was reported as <0.001, this was based on at least 10^6 simulations). (*iii*) The third assessment was by estimating the sampling SE of the VBE metric (see below) for each line using bootstrap resampling and calculating the P value associated with the null hypothesis that VBE = 0 using a z distribution. Bootstrap resampled estimates of VBE were always observed to follow Gaussian distributions.

Choice of VBE Metric. We considered a number of different ways of measuring behavioral variability beyond expectation. These are summarized in Table S3. Most metrics are $\log_2$-linearized because they are each the ratio of a measure of the dispersion of the observed distribution over that of the expected distribution. All metrics were highly correlated to one another across 117 of the experimental groups in this study (Table S4). Ultimately, we chose to use mean absolute deviation ratio (μADR) = $\log_2(\mu AD_{obs}/\mu AD_{exp})$, where μAD indicates the mean absolute deviation of the data within each sample from their median (3). This metric has the advantageous following properties: (*i*) sensitivity to outliers (because phototactic personality manifests as individuals with unusual behavior, metrics discarding the tails of sample distributions are not useful); (*ii*) it is nonparametric; (*iii*) fairly high signal-to-noise ratio in the context of bootstrap resampling; and (*iv*) with the highest correlation to all other metrics, it represents a "consensus metric." The primary disadvantage of this metric, low signal-to-noise ratio compared with SD ratio (SDR) and μLL (see Table S3 for definitions), was overcome by large sample sizes in each experimental group.

Statistical Comparison of VBE Metrics. Because the data from all animals in each experimental group were used to calculate each VBE score, we used 1,000 bootstrap-resampling replicates to

estimate the error associated with that metric. Error bars in Figs. 2 and 4–6 are ±1 SE, equal to the SD of the bootstrap-resampled estimates of VBE. Because there is, to our knowledge, no analytic formula for P values associated with differences in μADR, we calculated these numerically using the formula:

$$\int_{-\infty}^{\infty}\left(\mathcal{N}(\mu_1,\sigma_1^2)\int_{x_1}^{\infty}\mathcal{N}(\mu_2,\sigma_2^2)dx_2\right)dx_1,$$

where $\mu_1 > \mu_2$, and $N(\mu_i,\sigma_i^2)$ is the normal distribution, with mean μ and variance σ^2 equaling, respectively, the average bootstrap estimate of VBE and the variance of those estimates, for experimental group i. Because bootstrap resampling estimates of VBE were always found to be normally distributed, this yielded a one-tailed P value against the null hypothesis that $\mu_1 = \mu_2$. This formula was in complete agreement with resampling calculations in which we simply resampled VBE of group 1 and determined how frequently it was estimated as $<\mu_2$.

Additionally, we performed a resampling equivalent of ANOVA to test whether there was more variation within the groups of $[w^+]\rightarrow w^{501}$ and $[w^{501}]\rightarrow w^+$ introgression lines (Fig. 4*B*) than would be expected by chance, given a null hypothesis of identical VBE across these lines. Specifically, we randomly shuffled the data between the lines (e.g., $[w^+]\rightarrow w^{501}$) while preserving the samples sizes of each group, calculated new VBEs for each, and calculated the mean absolute deviation (MAD) of these shuffled VBEs. P values were determined by repeating this process and determining the fraction of time $\mathrm{MAD}(\mathrm{VBE}_{\mathrm{shuffled}}) > \mathrm{MAD}(\mathrm{VBE}_{\mathrm{original}})$. For $[w^+]\rightarrow w^{501}$, $P = 0.78$ based on 8,300 replicates; for $[w^{501}]\rightarrow w^+$, $P = 0.10$ based on 5675 replicates. This is consistent with *white* (or a locus/loci closely linked to it) being the only locus contributing to variation in the introgression lines.

Analysis of Environment-Matched Animals. We found that birth order affected the average probability with which flies chose to go toward the light (Fig. S2*B*; $P = 0.0033$ by three-way standard ANOVA considering the birth cohort, mother, and sex of each fly). The maximal difference in average light-choice probability between these groups was comparatively small (11%), and the statistical significance of this result is attributable to the high number of individuals assayed. Importantly, the apparent effect of birth order on phototactic preference cannot explain the total variability we see between individuals. Even if a population were composed in equal portions of animals choosing light 62% of the time and animals choosing light 51% of the time (the average light-choice probabilities of most and least phototactic egg batches, respectively), the observed variance is still greater than expected ($P < 0.0001$ by χ^2 test of variance). This implausibly conservative scenario explains at most 54% of the observed excess behavioral variance. Moreover, each of the birth cohort groups individually shows more variance than expected.

1. Francis JB (1855) *Lowell Hydraulic Experiments* (Allen and Farnham, Cambridge, MA).
2. Carpenter FW (1905) The Reactions of the Pomace Fly (Drosophila ampelophila Loew) to Light, Gravity, and Mechanical Stimulation. *Amer Naturalist* 39(459):157–171.
3. Huber PJ (1981) *Robust Statistics* (John Wiley & Sons, New York).

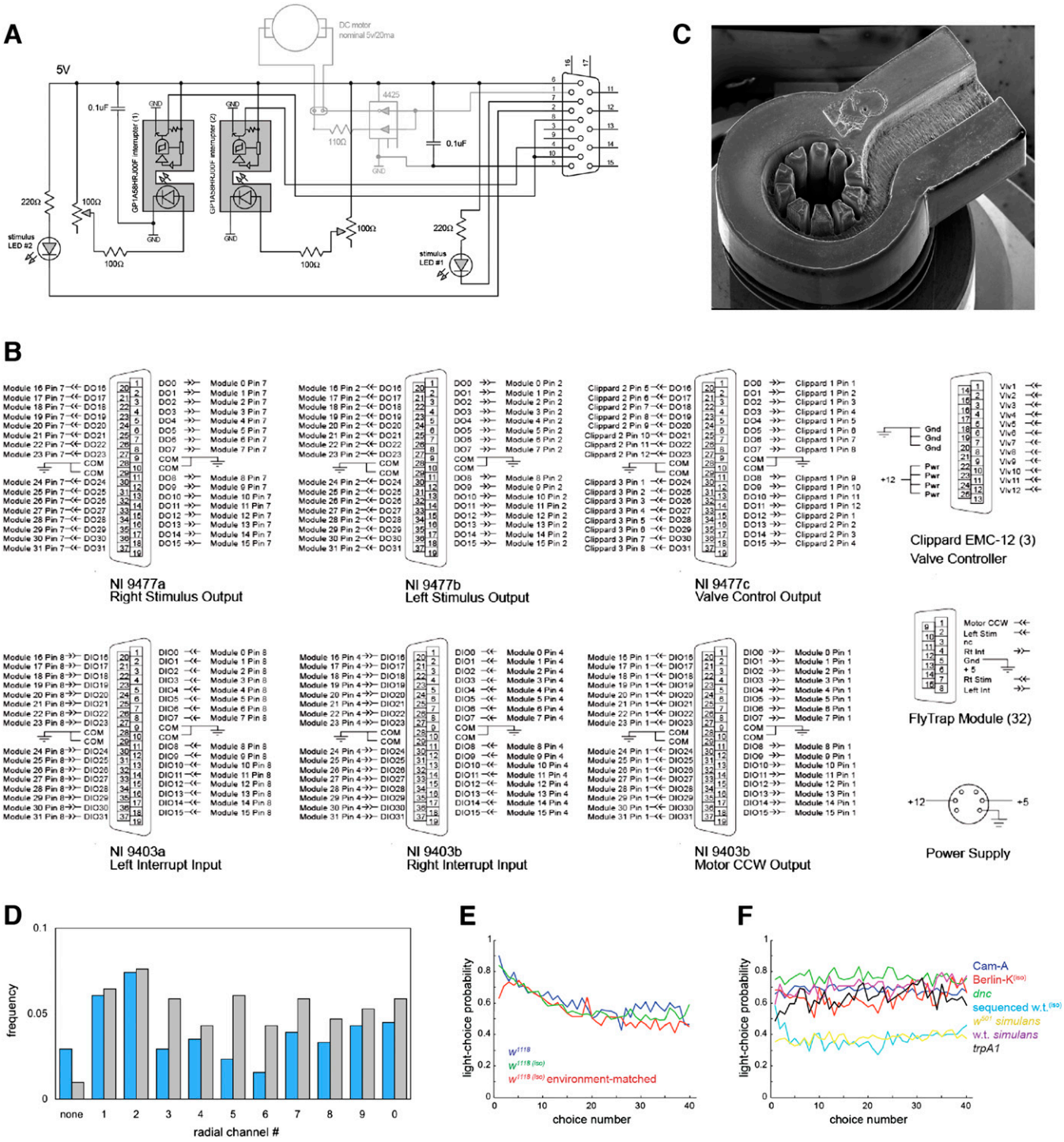

Fig. S1. FlyVac specifications and performance (Fig. 1). (*A*) Circuit diagram of FlyVac modules. Grayed-out components allow the FPGA to control the state of a motor/trap door system implemented in preliminary versions of the device but are dispensable in the device as reported. (*B*) Wiring diagram of FlyVac motherboard. (*C*) Mosaic of scanning-electron micrographs of the engraved half of a vacuum trap. The trap is 18 mm long, 12.5 mm wide, and 5.3 mm high. Spiral plenum and channels connecting the plenum to the start tube are ~2 mm deep. (*D*) Histogram of the position(s) of fly wings (blue) and legs (gray) within the vacuum trap during vacuum pulses. Radial channel 1 is the closest to the vacuum source, and 0 is the farthest. Data from two flies, exposed to 75 vacuum pulses (25 pulse sets) each. "None" indicates cases in which either wings or legs were drawn to the opening of no radial channels during a pulse (n = 219 and 293 for wings and legs, respectively). These distributions are fairly uniform, particularly that of the animals' legs, indicating that the vacuum trap is reorienting the flies in close to a uniform random distribution during each vacuum pulse. (*E*) Average light-choice probability across all individuals tested versus choice number. Experimental groups using w^{1118} or lines derived therefrom. (*F*) As in *E*, for other groups. An inbred line derived from the sequenced *D. melanogaster* reference strain showed variation in its light-choice probability as a function of trial number, like w^{1118} (*E*).

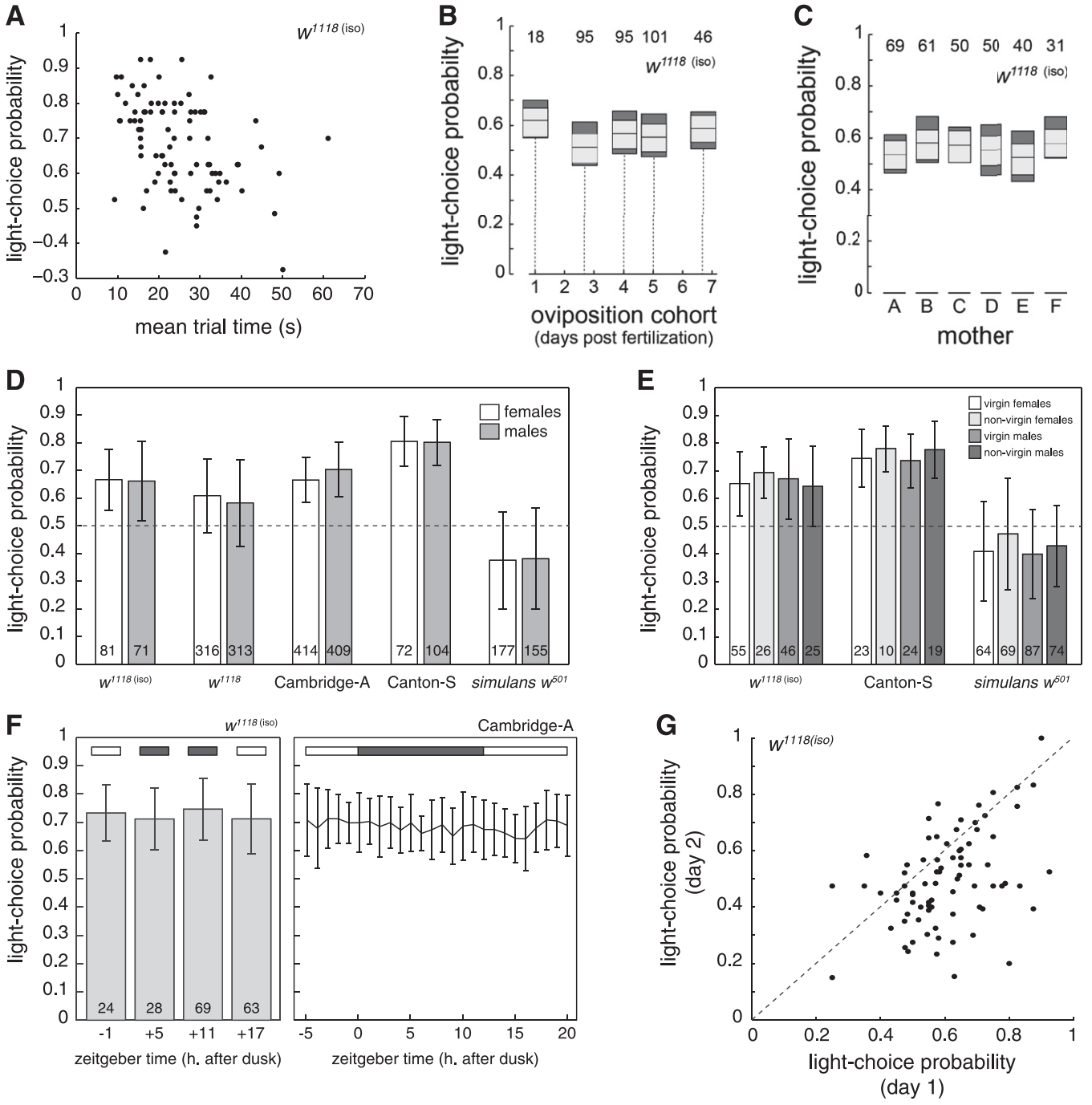

Fig. S2. Controls for variability beyond expectation. (*A*) Scatter plot of average trial completion time versus average light-choice probability ($r = -0.063$; $P = 0.44$) for $w^{1118\ (iso)}$ animals. The photonegativity of some individuals did not inhibit their completion of trials at typical rates. (*B*) Expected and observed IQRs (as in Fig. 2*G*) of environment-matched $w^{1118\ (iso)}$ grouped by birth order. Numbers above box plot indicate the sample size. (*C*) Expected and observed IQRs (as in Fig. 2*G*) of environment-matched $w^{1118\ (iso)}$ grouped by maternal identity. Numbers above box plot indicate the sample size. (*D*) Average light-choice probability of females and males for several representative strains. Error bars are ±1 SD. Numbers within each bar indicate sample size. (*E*) Average light-choice probability of virgin and nonvirgin females and males for several representative strains. Error bars are ±1 SD. Numbers within each bar indicate sample size. (*F*) Average light-choice probability versus circadian time for $w^{1118\ (iso)}$ ($P = 0.311$ by one-way ANOVA; numbers within each bar indicate sample size) (*Left*) and Cambridge-A flies ($P = 0.11$ by one-way ANOVA; sample size at each time point is 32 flies for most bars and >27 for all others) (*Right*). Error bars are ±1 SD. (*G*) Scatter plot of individual w^{1118} light-choice probabilities on day 2 versus day 1. Dashed line indicates perfect identity between testing sessions.

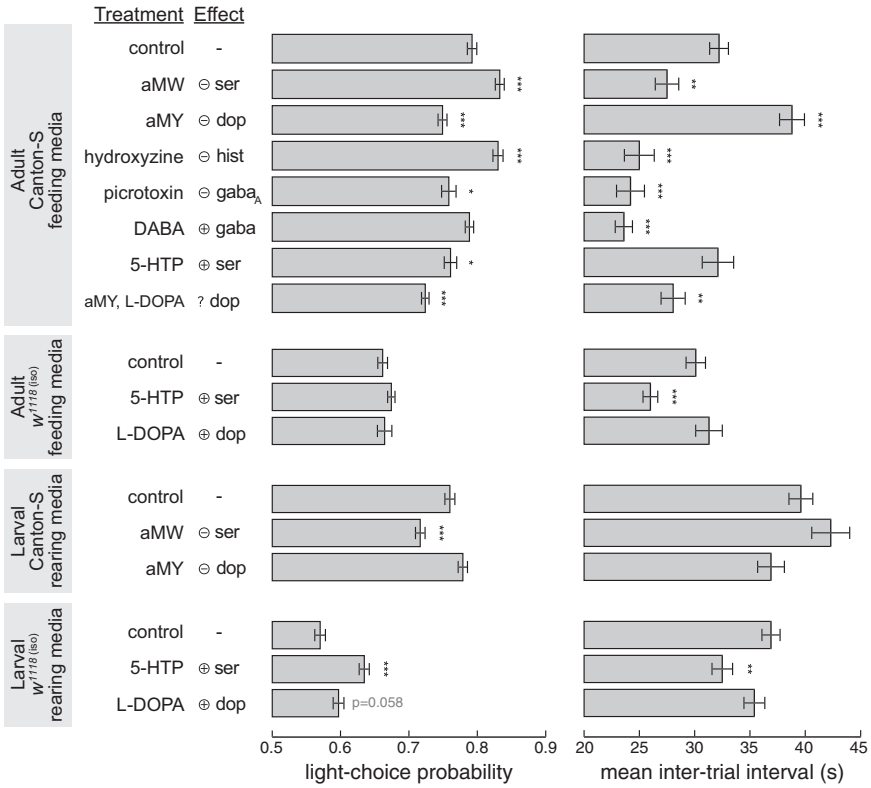

Fig. S3. Drug treatments have significant effects on light-choice probability and trial completion time. Average light-choice probabilities (*Left*) and mean intertrial intervals (*Right*) for the pharmacological experimental groups in Fig. 5. Error bars are 1 SEM, across flies. Asterisks indicate statistical significance versus respective control by *t* test, adjusted for four comparisons by Bonferroni correction: $*P < 0.05$; $**P < 0.01$; $***P < 0.001$. L-DOPA did not appear to have any significant effect on its own, although it caused a nearly significant decrease in light-choice probability in reared $w^{1118\,(iso)}$ larva. In combination feeding of Canton-S adults with L-DOPA and aMY, L-DOPA did not rescue the decrease in light-choice probability brought about by aMY feeding but did rescue the increase in intertrial times caused by aMY, with very high statistical significance.

Table S1. List of strains analyzed, their genotypes and sources

	Strain label	Species	Fig(s).	Genotype	Source
1	Canton-S	*D. melanogaster*	1, 2, and 5–7	Wild type	W. Quinn (MIT)
2	w^{1118}	*D. melanogaster*	2	w^{1118}	J. Dubnau (CSHL)
3	Cambridge-A	*D. melanogaster*	2	Wild type	This work
4	*norpA*	*D. melanogaster*	2	*norpA*	BSC
5	w^{501} *simulans*	*D. simulans*	2, 4, and 5	w^{501}	DSSC no. 14021-0251.195
6	*I. virens.*	*Ischnopterapion virens*	2	Wild type	This work
7	Wild-type *pseudoobscura*	*D. pseudoobscura*	2	Wild type	DSSC no. 14011-0121.101
8	Wild-type *simulans*	*D. simulans*	2 and 5	Wild type	DSSC no. 14021-0251.194
9	Arlington-B	*D. simulans*	2	Wild type	This work
10	Cambridge-A$^{(iso)}$	*D. melanogaster*	2	Wild type	This work
11	Boston-A	*D. melanogaster*	2	Wild type	This work
12	Somerville-A	*D. melanogaster*	2	Wild type	This work
13	Berlin-K$^{(iso)}$	*D. melanogaster*	2	Wild type	This work
14	$w^{1118\ (iso)}$	*D. melanogaster*	2, 3, 5, and 6	w^{1118}	This work
15	$[w^{+}]\rightarrow w^{501}$	*D. simulans*	4	14021-0251.*195*-$Int_{10}(1)w^{+}$	This work
16	$[w^{501}]\rightarrow w^{+}$	*D. simulans*	4	14021-0251.*194*-$Int_{10}(1)w^{501}$	This work
17	w^{1118}; +/+	*D. melanogaster*	4	w^{1118}-$Int_1(2)w^{1118}$	This work
18	w^{1118}; +/ $\{w^{+mW.hs}\}$	*D. melanogaster*	4	w^{1118}-$Int_1(2)w^{+mW.hs}$	This work
19	*brown*	*D. melanogaster*	4	bn^1	BSC
20	*scarlet*	*D. melanogaster*	4	st^1	BSC
21	*cinnabar*	*D. melanogaster*	4	cn^1	BSC
22	$[w^{+}]\rightarrow w^{1118\ (iso)}$	*D. melanogaster*	4	$w^{1118\ (iso)}$-$Int_{10}(1)w^{+}$	This work
23	$[w^{1118\ (iso)}]\rightarrow w^{+}$	*D. melanogaster*	4	Canton-S-$Int_{10}(1)w^{1118\ (iso)}$	This work

For the introgression notation, "*B-Int$_A$(C)D (E)*" indicates an A-generation introgression (*Int$_A$*) into the B genetic background, selecting for the D marker, which resides on chromosome C. E is the source strain of marker D, if D is transgenic. BSC, Bloomington Stock Center; DSSC, *Drosophila* Species Stock Center.

Table S2. List of drugs used, their concentrations, and references

Drug	Final concentration	Ref.	Notes
aMY	2.6 mM	1	—
aMW	20 mM	2	Ascorbic acid (25 mg per 100 mL) was added as a stabilizer
Hydroxyzine	27 mM	3	Approximately half the flies die after 5 d of exposure at this concentration
L-DOPA	5.1 mM	4	—
5-HTP	50 mM	2	—
DABA	26 mM	5	Stock concentration in DMSO; approximately half of the flies die after 5 d of exposure at this concentration
Picrotoxin	3.3 μM	6	Stock concentration in DMSO; approximately half the flies die after 5 d of exposure at this concentration

1. Sitaraman D, et al. (2008) Serotonin is necessary for place memory in Drosophila. *Proc Natl Acad Sci USA* 105(14):5579–5584.
2. Dierick HA, Greenspan RJ (2007) Serotonin and neuropeptide F have opposite modulatory effects on fly aggression. *Nat Genet* 39(5):678–682.
3. Shaw PJ, Cirelli C, Greenspan RJ, Tononi G (2000) Correlates of sleep and waking in Drosophila melanogaster. *Science* 287(5459):1834–1837.
4. Bainton RJ, et al. (2000) Dopamine modulates acute responses to cocaine, nicotine and ethanol in Drosophila. *Curr Biol* 10(4):187–194.
5. Leal SM, Neckameyer WS (2002) Pharmacological evidence for GABAergic regulation of specific behaviors in Drosophila melanogaster. *J Neurobiol* 50(3):245–261.
6. Leal SM, Kumar N, Neckameyer WS (2004) GABAergic modulation of motor-driven behaviors in juvenile Drosophila and evidence for a nonbehavioral role for GABA transport. *J Neurobiol* 61(2):189–208.

Table S3. Comparison of metrics for VBE

Metric	Formula	Nonparametric	Sensitive to tails	Stability
IQRR	$\log_2\left(\frac{\mathrm{CDF}_{\mathrm{obs}}^{-1}(0.75)-\mathrm{CDF}_{\mathrm{obs}}^{-1}(0.25)}{\mathrm{CDF}_{\mathrm{exp}}^{-1}(0.75)-\mathrm{CDF}_{\mathrm{exp}}^{-1}(0.25)}\right)$	Yes	No	6
SDR	$\log_2\left(\frac{s_{\mathrm{obs}}}{\sigma_{\mathrm{exp}}}\right)$	No	Yes	9.6
μADR	$\log_2\left(\frac{\frac{1}{N_{\mathrm{obs}}}\sum\lvert x_{\mathrm{obs}}-\mathrm{CDF}_{\mathrm{obs}}^{-1}(0.5)\rvert}{\int \mathrm{PDF}_{\mathrm{exp}}(x)\lvert x-\mathrm{CDF}_{\mathrm{exp}}^{-1}(0.5)\rvert dx}\right)$	Yes	Yes	8.4
MADR	$\log_2\left(\frac{\mathrm{median}(\lvert x_{\mathrm{obs}}-\mathrm{CDF}_{\mathrm{obs}}^{-1}(0.5)\rvert)}{\mathrm{median}(\lvert x_{\mathrm{exp}}-\mathrm{CDF}_{\mathrm{exp}}^{-1}(0.5)\rvert)}\right)$	Yes	No	ND
μLL	$-\frac{1}{N_{\mathrm{obs}}}\log\left(\prod\binom{n_i}{k_i}p_{\mathrm{obs}}^{k_i}(1-p_{\mathrm{obs}})^{1-k_i}\right)$	No	Yes	171

CDF, cumulative distribution function of the observed (obs) or expected (exp) distributions; IQRR, IQR ratio; k_i, number of choices made by fly i toward the light; μADR, mean absolute deviation ratio; μLL, mean log likelihood; σ, SD; MADR, median absolute deviation ratio; n, sample size; ND, not determined; n_i, number of choices made by fly i; PDF, probability distribution function; p_{obs}, average light-choice probability observed across flies; s, sample SD; SDR, SD ratio; x_{exp}, numerically computed light-choice probabilities of simulated flies having the distributed $\mathrm{PDF}_{\mathrm{exp}}$ distribution; x_{obs}, light-choice probabilities of individual flies. Stability was calculated as the mean, across experimental groups of each metric's value divided by the SE of its estimated value across bootstrap resamples.

Table S4. Correlation coefficient of VBE metrics across 117 experimental groups in this study

	IQRR	SDR	μADR	μLL	MADR
IQRR	1	0.95	0.98	0.89	0.87
SDR	0.95	1	0.98	0.90	0.86
μADR	0.98	0.98	1	0.92	0.88
μLL	0.89	0.90	0.92	1	0.86
MADR	0.87	0.86	0.88	0.86	1
mean	0.94	0.94	0.95	0.92	0.89

The μADR metric used in the main text showed the greatest mutual agreement with the other (mean $r = 0.95$).

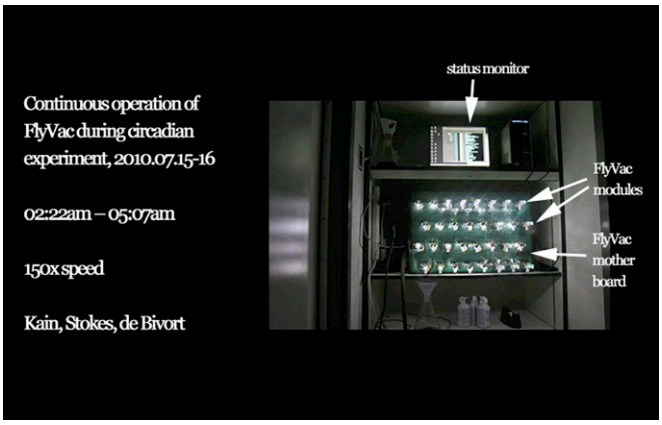

Movie S1. Movie illustrating the use of FlyVac during the Cambridge-A circadian experiment (Fig. S2*F*) and meant to give a general impression of the appearance and use of FlyVac. For example, at 00:21, a synchronized time point is initiated with the activation of all modules. Data collection proceeds for 45 min, at which point the data are saved, and the flies are removed and replaced before the next time-point experiment. The movie portrays nearly 3 h of use. Frames were acquired every 5 s. Playback is at 30 frames per second (fps).

Movie S1

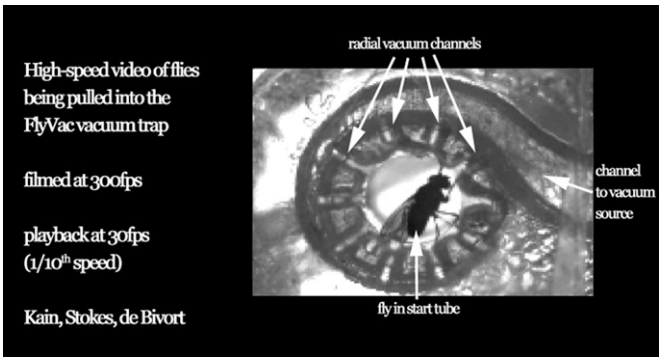

Movie S2. Flies being sucked into the vacuum trap. A trap was assembled with a sealed, clear-bottom replacing the flow-regulating screen, to allow visualization of flies being sucked into the trap. The bright circle at center is the start tube, viewed end-on. Ten radial channels connect the start tube to the Francis plenum, which spirals clockwise and exits the frame on the right. This is the path of airflow out of the vacuum trap. Flies start each segment in the choice tubes and out of frame, or in frame but out of focus. Vacuum pulses pull them into the start tube and into focus. After the pulses, the flies regain their footing and begin to walk upward out of the trap. (It should be noted that replacing the flow-regulating screen for the purposes of video increased the intensity of the vacuum pulse; thus, flies in actual experimental groups experienced less violent vacuum than seen in the movie.) The movie was recorded at 300 fps and is played back at 30 fps. Four representative examples of fly motion into the trap and recovery are provided.

Movie S2

Dataset S1. Tab-delimited text file of raw phototactic choice data across experimental groups

Dataset S1 (TXT)